

IDC Sensor Report

Cannizzo Emanuele, Di Mauro Miriam, and Finocchiaro Carla

Automation Engineering and Control of Complex Systems - DIEEI - *Università degli Studi di Catania*

May 31, 2024

Abstract

This report presents a comprehensive study on interdigital capacitor (IDC) sensors, covering both theoretical modeling and practical implementations. The Kim model, which utilizes conformal mapping technique, is employed to calculate the capacitance of planar IDC sensor, with results validated through MATLAB simulations. Key parameters such as layer thickness and dielectric permittivity are varied to analyze their influence on sensor sensitivity. The study also includes the fabrication of IDC sensors using inkjet printing technology, followed by detailed electrical and morphological characterizations. Capacitance and resistance measurements are reported, demonstrating the accuracy and reliability of the fabricated sensors. Furthermore, the implementation of conditioning electronics using an AC Wheatstone bridge is described, which allows for the conversion of capacitance variations into measurable voltage changes, thus enhancing the sensor's application potential. The MATLAB code used for conducting the simulation and analysis is available on a Github repository [1].

Contents

1 Kim Model	2
2 Simulations	2
2.1 Simulation of a Bare IDC	2
2.2 Simulation of an IDC with a Second Layer	3
3 Measure Session	3
3.1 Electrical characterization	4
3.2 Morphological characterization	6
4 Conditioning Electronic Characterization	7
References	9

1 Kim Model

The Kim Model [2] uses the conformal mapping technique to exploit the capacitance of a planar sensor. This technique allows to map the planar structure of the IDC capacitor, through a series of conformal maps, into a parallel plate capacitor. Then the partial capacitance method is used to combine together all the partial capacitance given by each layer. The generic capacitance of the i^{th} layer is calculated as:

$$C_i = 2\epsilon_0\epsilon_i \frac{K(k'_i)}{K(k_i)} \quad (1)$$

where k'_i is:

$$k'_i = \frac{\sinh \frac{\pi b}{4h_i}}{\sinh \left[\frac{\pi}{2h_i} \left(\frac{b}{2} + d \right) \right]} \dots$$

$$\sqrt{\frac{\sinh^2 \left[\frac{\pi}{2h_i} \left(\frac{b}{2} + d + a \right) \right] - \sinh^2 \left[\frac{\pi}{2h_i} \left(\frac{b}{2} + d \right) \right]}{\sinh^2 \left[\frac{\pi}{2h_i} \left(\frac{b}{2} + d + a \right) \right] - \sinh^2 \left(\frac{\pi b}{4h_i} \right)}}$$

k_i is: $\sqrt{1 - k'^2}$ and $a = \frac{b}{2}$. Then the total capacitance in the case of a three layers IDC capacitor showed in Figure 1 is calculated as:

$$C_{idc} = nl(C_1 + C_2 + C_3) \quad (2)$$

where:

- C_1 is the line capacitance (per unit length) of the interdigitated electrodes with Layer 1 only (thickness h_1 , permittivity ϵ_1);
- C_2 is the line capacitance (per unit length) of the interdigitated electrodes with Layer 2 only (thickness h_2 , permittivity $\epsilon_2 - \epsilon_3$);
- C_3 is the line capacitance (per unit length) of the interdigitated electrodes with Layer 3 only (thickness $h_2 + h_3$, permittivity ϵ_3).

Moreover it was found via simulations that:

- to neglect the capacitance C_2 due to second layer it's sufficient to set its thickness to a value smaller than $10\mu\text{m}$;
- to neglect the capacitance C_3 it's sufficient to impose $h_2 + h_3 < 20\mu\text{m}$;
- h_2 cannot have values less than $1\mu\text{m}$ because the model used for simulation generates an exception;

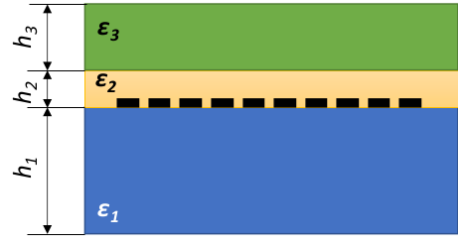


Figure 1: 2D schematic of a 3-layers IDC sensor.

2 Simulations

2.1 Simulation of a Bare IDC

The first MATLAB simulation was conducted considered only the substrate on which the IDC sensor was printed, which is PET. Two different models were used: the Kim Model and an Interdigital Capacitor model provided by a MATLAB package [3]. The parameters used in the simulation are listed in Table 1 and Table 2. In addition, the parameters required by the MATLAB implementation are reported in Table 3. The capacitance obtained through the Kim's model is 0.6076 pF , while the capacitance obtained using the MATLAB model is 0.57872 pF . It can be concluded that the two models exhibit a high degree of coherence. In this case, they differ by approximately 30 pF .

Parameter	Value (mm)
n	6
l	5
b	0.3
d	0.3

Table 1: IDC set values during inkjet printing. **n** is the number of finger pairs, **l** is the overlapping finger length, **b** is the finger width, and **d** is the finger spacing.

Parameter	Value
h1 (μm)	140
h2 (μm)	10
h3 (μm)	10
eps1 (F/m)	3.5
eps2 (F/m)	1
eps3 (F/m)	1

Table 2: **h1**, **h2**, and **h3** are the dielectric thicknesses, while **eps1**, **eps2**, and **eps3** are the corresponding permittivities.

Parameter	Value
FingerEdgeGap (mm)	0.5
TerminalStripWidth (mm)	1
PortLineWidth (mm)	1
PortLineLength (mm)	9
GroundPlaneWidth (mm)	6.9
Height (mm)	1000
Conductor	"metal"
Operating Bandwidth (kHz)	20

Table 3: For more information about these parameters refer to [3].

2.2 Simulation of an IDC with a Second Layer

In this stage, the IDC sensor was simulated with a layer placed on top of the substrate. The layer considered in this simulation is Polydopamine. For this simulation and all subsequent ones, only the Kim Model was used, due to the fact that the MATLAB model can simulate only a single-layer IDC (i.e., only the substrate). The new parameters related to the second layer are listed in Table 4. The obtained capacitance is 0.96589 pF.

Parameter	Value
h1 (μm)	140
h2 (μm)	1000
h3 (μm)	10
eps1 (F/m)	3.5
eps2 (F/m)	1.23
eps3 (F/m)	1

Table 4: h1, h2, and h3 are the dielectric thicknesses, while eps1, eps2, and eps3 are the corresponding permittivities.

Dielectric Thickness Sensitivity Analysis

The sensitivity of the IDC sensor was tested in response to variations in the thickness of the second layer. The values tested range from a minimum of $3 \mu\text{m}$ to a maximum of $1200 \mu\text{m}$, corresponding to λ , with a step of $3 \mu\text{m}$. As shown in Figure 2, if the dielectric thickness exceeds $\frac{\lambda}{2}$, the capacitance tends to saturate, as predicted by the theory of IDC sensors. To achieve a linear response and quasi-constant responsivity, it is advisable to work with a layer thickness not exceeding $200 \mu\text{m}$. Additionally, for thicknesses smaller than $15 \mu\text{m}$, the capacitance is insensitive to the thickness of the second layer.

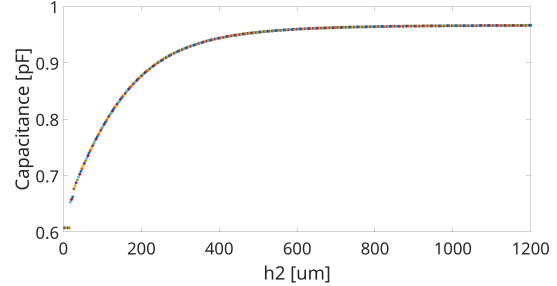


Figure 2: Dielectric thickness sensitivity analysis.

Dielectric Thickness and Permittivity Sensitivity Analysis

To have a more precise characterization of the sensor, it was conducted a mixed analysis varying not only the thickness but also the permittivity of the dielectric layer. The thickness varies from a minimum of 0.1 mm to a maximum of λ , with a step of 0.1 mm . The dielectric permittivity varies from a minimum of 0.7 F/m to a maximum of 4 F/m , with a step of 0.2 F/m . As shown in Figure 3, the responsivity with respect to the permittivity increases as the second layer thickness increases. Thus, it may seem that the optimal region of operation is the one with the greatest thickness.

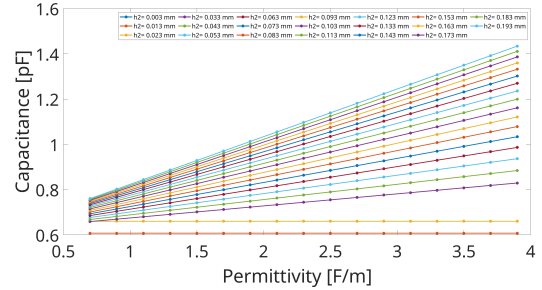


Figure 3: Dielectric thickness and permittivity sensitivity analysis.

3 Measure Session

In this session, several sensors were printed to test how much the predictions deviate from the values extracted from the actual sensors. The sensors were printed using the Dimatix Materials DMP-2850, which employs the inkjet printing technique.

3.1 Electrical characterization

Resistive Measurements

To evaluate the resistive paths in the IDC sensor, a reduced version was designed, containing only one pad, the corresponding finger, and the ribbon (Figure 4).

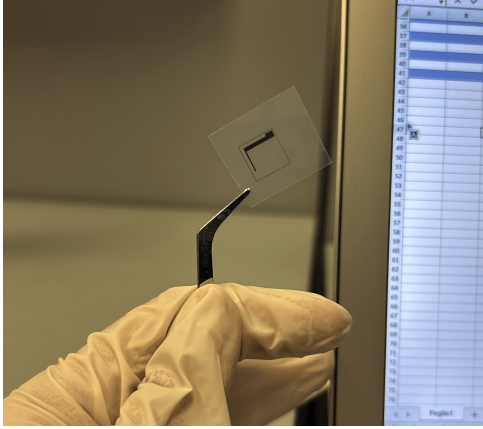


Figure 4: Reduced version of sensor for resistance measurements.

Measurements were performed ten times on the same sensor, in the following order to ensure better repeatability and reliability: ribbon-ribbon resistance, finger-finger resistance, and ribbon-finger resistance. The results are shown in Figure 5, Figure 9, Figure 7.

As can be seen from Figure 6, the ribbon of device 6 has an high value of standard deviation, about three times bigger than the smallest one. From Figure 8 it can be seen that the measurements of the ribbon-finger path are very close one to another. Finally, Figure 10 shows that device 1 has a value of standard deviation relative to the finger path from five to eighteen times bigger than others. This suggests a damage in the device during the measurements.

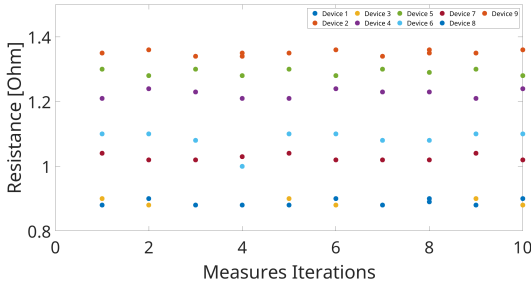


Figure 5: Ribbon-Ribbon resistance of the reduced version device

Device	Mean (Ω)	Std (Ω)
Device 1	0.8	0.0095
Device 2	1.35	0.0082
Device 3	0.888	0.0103
Device 4	1.2250	0.0135
Device 5	1.291	0.0099
Device 6	1.084	0.0310
Device 7	1.0270	0.0095
Device 8	0.888	0.0103
Device 9	1.3520	0.0079

Table 5: Mean and Standard Deviation relative to the Ribbon-Ribbon resistance.

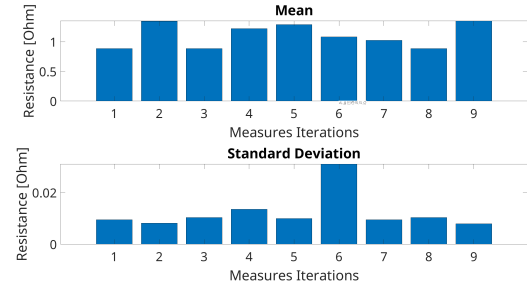


Figure 6: Mean and Standard Deviation relative to the Ribbon-Ribbon measurements listed in Table 5).

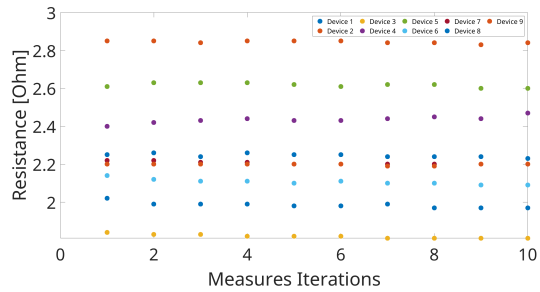


Figure 7: Ribbon-Finger resistance of the reduced version device.

Device	Mean (Ω)	Std (Ω)
Device 1	1.9850	0.0151
Device 2	2.8440	0.0070
Device 3	1.82	0.0105
Device 4	2.4350	0.0184
Device 5	2.6170	0.0116
Device 6	2.1070	0.0149
Device 7	2.2060	0.0084
Device 8	2.2460	0.0097
Device 9	2.1980	0.0042

Table 6: Mean and Standard Deviation relative to the Ribbon-Finger resistance.

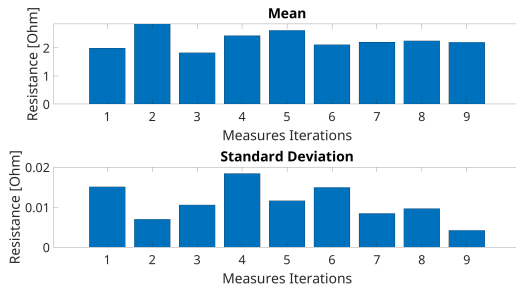


Figure 8: Mean and Standard Deviation relative to the Ribbon-Finger measurements listed in Table 6).

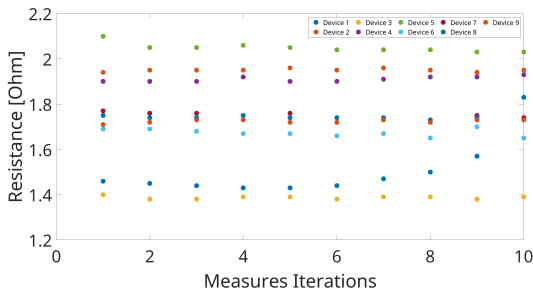


Figure 9: Finger Finger resistance of the reduced version device.

Device	Mean (Ω)	Std (Ω)
Device 1	1.5020	0.1228
Device 2	1.9500	0.0067
Device 3	1.3870	0.0067
Device 4	1.9100	0.0115
Device 5	2.049	0.0202
Device 6	1.673	0.0170
Device 7	1.75	0.0125
Device 8	1.74	0.0067
Device 9	1.724	0.0070

Table 7: Mean and Standard Deviation relative to the Finger-Finger resistance.

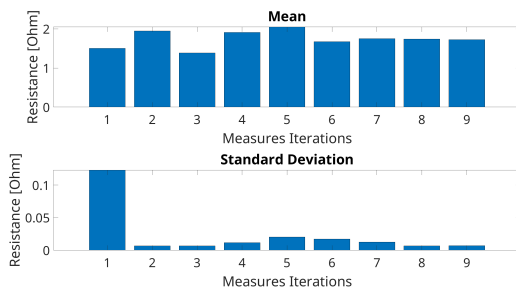


Figure 10: Mean and Standard Deviation relative to the Finger-Finger measurements listed in Table 7).

Capacitance Measurements

For the capacitance measurements, ten identical IDC sensors were printed, and the capacitance of each sensor was measured using an LCR meter. Since the capacitance in question are on the order of magnitude of pF , the setup shown in Figure 11 was specifically designed to ensure accurate and reliable measurements. A shielded cable with a braid was employed to reduce electromagnetic interference. Additionally, the sensor was elevated above the workbench to further minimize any potential disturbances from the surrounding environment.

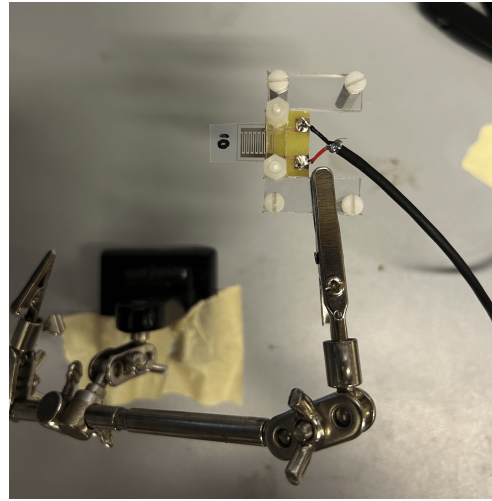


Figure 11: Setup for capacitance measurements.

Measurements were performed ten times on the same sensor and the results are shown in Figure 12. Figure 13 displays the mean and standard deviation of the capacitance measurements. It is evident that, except for the first device, the mean values are quite similar. Observing as well the standard deviation of the first device, that is quite small, it can be concluded that its different behaviour in terms of capacitance is due to a printing error.

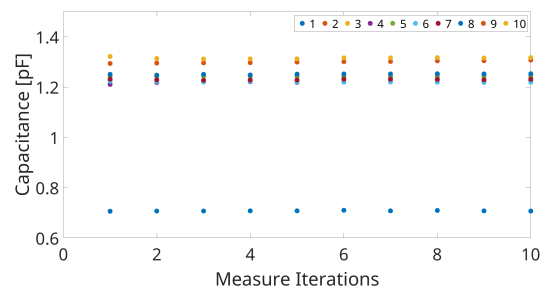


Figure 12: Capacitance measurements of the bare sensors.

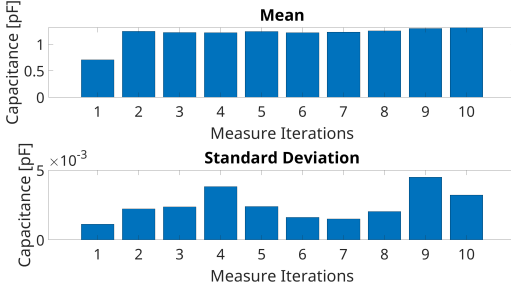


Figure 13: Mean and Standard Deviation relative to the capacitance measurements listed in Table 8.

Device	Mean (pF)	Std (pF)
Device 1	0.7078	0.0011
Device 2	1.2434	0.0022
Device 3	1.2235	0.0024
Device 4	1.2193	0.0038
Device 5	1.2412	0.0024
Device 6	1.2202	0.0016
Device 7	1.2295	0.0015
Device 8	1.2508	0.0020
Device 9	1.3	0.0045
Device 10	1.3152	0.0032

Table 8: Mean and Standard Deviation relative to the capacitance measurements.

A parameter fine-tuning procedure was conducted to determine the actual values of the IDC sensor parameters. The first test focused on the parameters of the first layer, varying the dielectric constant while maintaining a fixed thickness value, and repeating the test for eleven different thickness values (Figure 14). The second test was performed similarly, focusing on the morphological parameters by varying the finger width while keeping the finger spacing constant. This procedure was repeated for 21 different finger spacing values (Figure 15). The parameter values obtained in the two preceding analyses are not realistic. This significant discrepancy in prediction is attributed to the measurement setup previously discussed. Specifically, the presence of air, parasitic capacitance from the probes, and potential inaccuracies in the calibration of the measurement instrument contribute to this mismatch.

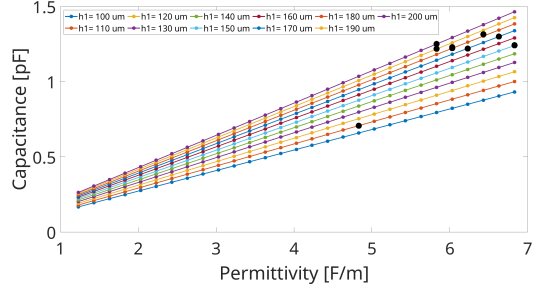


Figure 14: The graph illustrates how the capacitance varies with respect to h_1 and ϵ_1 . The black dots represent the actual capacitance values obtained during the measurement session. These dots are positioned at the points on the curve where the best matching occurs.

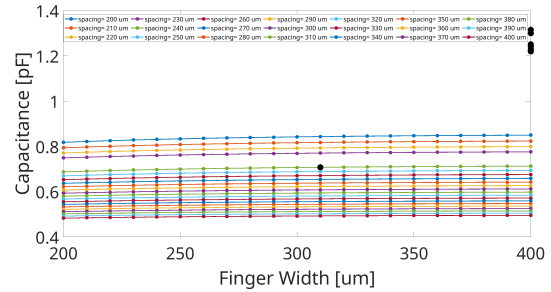


Figure 15: The graph illustrates how the capacitance varies with respect to the finger spacing d and the finger width b . The black dots represent the actual capacitance values obtained during the measurement session. These dots are positioned at the points on the curve where the best matching occurs.

3.2 Morphological characterization

The dimensions of the 10 sensors on which resistance and capacitance measurements were conducted, were measured using the Dimatix Materials DMP-2850 printer. This was done to refine Kim's model and determine if the capacitance values align more closely with the real values by using the parameters measured on the actual sensors. The dimensional parameters of interest are those required by the model:

- **Overlapping finger length** evaluated as the difference between the full length of the finger (Figure 16) and the distance between the finger and the ribbon (Figure 17).
- **Finger width** (Figure 18)
- **Finger spacing** evaluated by subtracting the width of the finger (Figure 18) from the distance between two fingers of the same ribbon (Figure 19) and dividing by two.

Parameter	Value (μm)
l	4998.1
b	299.70
d	287.85

Table 9: mean values of measured IDC parameters. **l** is the overlapping finger length, **b** is the finger width, and **d** is the finger spacing.

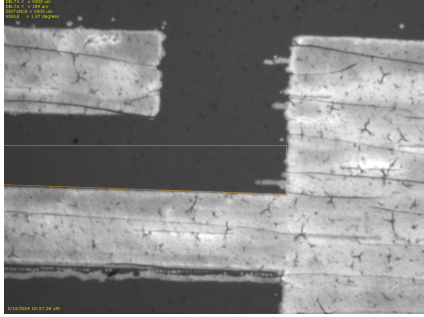


Figure 16: Finger length.

The mean value obtained from the results, are reported in Table 9. Compared to the initial parameters inserted into the model (Table 1), the dimensions of overlapping finger length and width remain largely unchanged; however, the most notable variation occurs in the spacing between the fingers. Using the initial parameters, it was achieved a capacitance (in the case of bare IDC) of 0.6076 pF . By incorporating the previously listed parameters, a capacitance of 0.6251 pF was obtained. As expected, the capacitance has varied due to changes in the geometrical properties of the sensors.

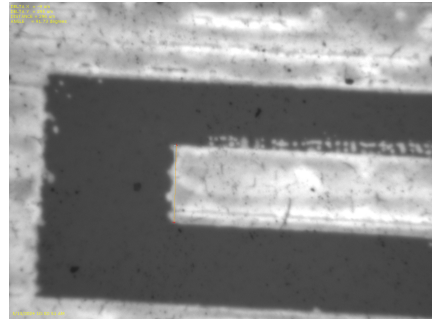


Figure 18: Finger width.

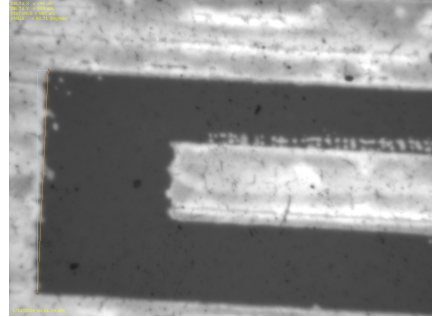


Figure 19: Distance between two fingers of the same ribbon.



Figure 17: Distance between finger and ribbon.

4 Conditioning Electronic Characterization

To convert the capacitance measurement into a voltage measurement, conditioning electronics are required. For this purpose, an AC Wheatstone bridge in a differential configuration was designed (Figure 20), utilizing a dummy sensor. The dummy sensor is identical to the actual sensor, with the crucial distinction that while the actual sensor responds to the measured variable (dielectric variation) as well as all external factors, the dummy sensor only responds to external factors. This design ensures that the output of the bridge represents the difference between the actual sensor and the dummy sensor, effectively canceling out any interference that affects both sensors equally.

However, even with identical manufacturing processes, there can be slight variations in the impedances of the actual and dummy sensors. To compensate for these discrepancies, a potentiometer is included across the two resistors in the bridge. This potentiometer allows for fine adjustment of the bridge's balance, ensuring that in the absence of the target variable (i.e., when no dielectric variation is present), the output voltage of the bridge is zero. This balancing procedure is crucial as it sets a stable baseline for the system, eliminating any offset that might arise from inherent sensor differences.

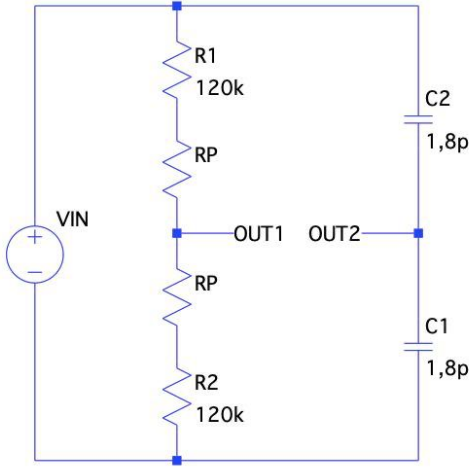


Figure 20: Conditioning electronics schematic.

The electronic was obtained from a PCB board (Figure 21) through a milling process. To test the electronic, instead of the two IDC sensors, two fixed value capacitors were used. One capacitor emulates the dummy sensor, the other is putted in parallel with another known capacitance to simulate the effect of the target quantity increasing the capacitance. This last capacitance was constructed creating a battery of a series of capacitance (Figure 22), to obtain capacitance variations in the order of picoFarads.

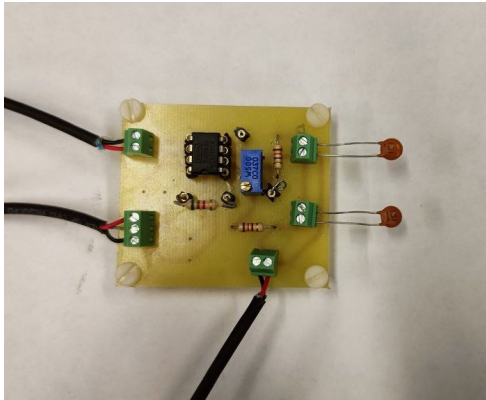


Figure 21: Conditioning electronics.

The values chosen for the components are:

- Fixed resistor of 120Ω ;
- Fixed capacitors of $1.8pF$;
- Potentiometer of 50Ω ;
- Series of 9 $1.8pF$ capacitance (Figure 22);
- Series of 2 $10pF$ capacitance.

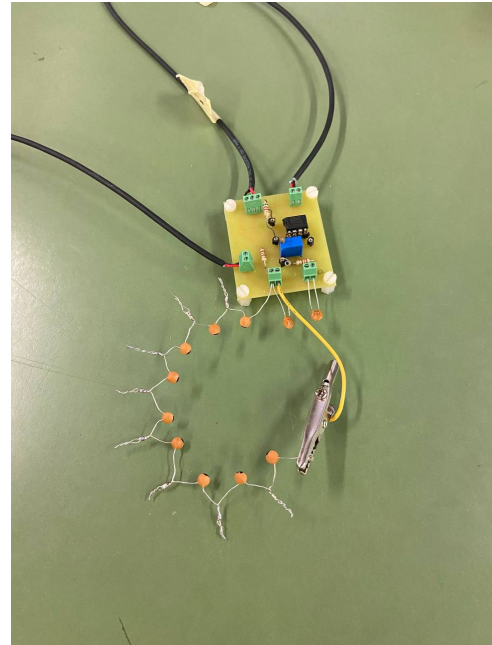


Figure 22: Series of $1.8pF$ capacitance.

To amplify the signal an INA111 high speed, FET-input instrumentation amplifier was employed, imposing a gain of 2. The calibration procedure was done by balancing the bridge with the potentiometer when no capacitance were added in parallel to the sensing one. Instead of achieving a perfect balance, which corresponds to a net $0V$, an offset of $0.7V$ was left. This was done to increase the robustness of the signal.

The measurements were done by moving the alligator clamp on to the series-battery, and taking note of the input capacitance and output voltage. This measure was done 5 times for each capacitance value. Moreover, the capacitance were evaluated using the LCR meter. The result of this measure session can be seen in Figure 23.

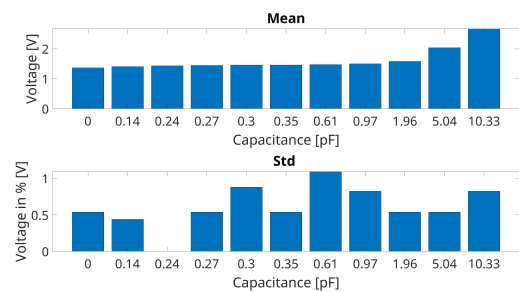


Figure 23: Mean and standard deviation of the voltage measurements taken with the conditioning electronics. The standard deviation is expressed as a percentage of the average voltage values.

First the means respect to each capacitance were evaluated. Then the standard deviation were ex-

Capacitance	Mean (V)	Std (V%)
0	1.3686	0.54
0.14	1.4092	0.4409
0.24	1.4370	0
0.27	1.4466	0.54
0.3	1.4594	0.8818
0.35	1.4626	0.5400
0.61	1.4750	1.0945
0.97	1.5032	0.8248
1.96	1.5844	0.54
5.04	2.0374	0.54
10.33	2.6688	0.8248

Table 10: Mean and standard deviation of the voltage measurements represented in Figure 23

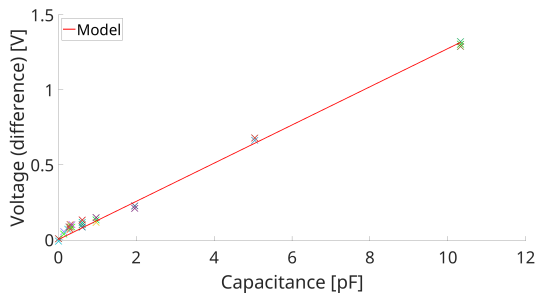


Figure 24: Trasduction Diagram.

pressed in percentage respect to the mean of the mean of all voltage readings done. From this last analysis it can be concluded that each measure it's very reliable, deviating at maximum of about 1% of the mean value. By dividing the standard deviation by the mean value and averaging these values across all capacitance measurements, a repeatability coefficient of 0.61% was found.

Lastly the trasduction (Figure 24) and calibration (Figure 25) diagrams were generated fitting the acquired data to a straight line passing through the origin. The uncertainty band was determined by considering two times the standard deviation of the residuals, which are calculated as the differences between each observed measurement and the corresponding predicted value from the model. This approach ensures that the uncertainty band covers a significant portion of the residuals. Additionally, no instrumentation uncertainty was included. It can be concluded that not only the device has a linear behaviour, but also the responsivity is quite constant in this working range.

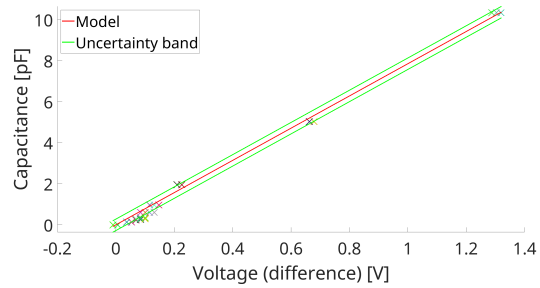


Figure 25: Calibration Diagram.

References

- [1] Idclaboratory. URL <https://github.com/manuele09/IDCLaboratory>.
- [2] Jun Wan Kim. *Development of Interdigitated Capacitor Sensors for Direct and Wireless Measurements of the Dielectric Properties of Liquids*. Ph.d. dissertation, The University of Texas at Austin, Austin, Texas, December 2008.
- [3] The MathWorks Inc. Rf pcb toolbox (interdigitalcapacitor), version: 23.2 (r2023b). URL <https://it.mathworks.com/help/rfpcb/ref/interdigitalcapacitor.html>.